



# SINTERING ANALYSIS OF 8YSZ ELECTROLYTE CORRELATED TO THE ELECTRICAL PERFORMANCE <sup>1</sup>

Cristiane Abrantes da Silva <sup>2</sup>  
Paulo Emílio Valadão de Miranda <sup>3</sup>  
José Geraldo de Melo Furtado <sup>4</sup>

## Abstract

The understanding of the mechanisms associated with densification and sintering of yttria stabilized zirconia (YSZ), a main solid oxide fuel cell electrolyte, enables the improvement of its microstructure. The present work that has the objective to study the sintering and densification processes of polycrystalline nanostructured 8% mol YSZ (8YSZ), correlating the microstructural development with the electrical performance of the material. The sintering behaviors of nanocrystalline 8YSZ powders obtained by two different chemical synthesis techniques (glycine-nitrate combustion process and Pechini method) were studied based on sintering dilatometer method. X-ray diffraction and scanning electron microscopy were used in the microstructural characterization. Full-densified 8YSZ (98.8%) were obtained and it was found that the samples obtained by the Pechini's method showed a higher densification degree in the final stage of sintering and resulted in ceramics with higher final relative density and better electrical behavior.

**Key words:** Yttria stabilized zirconia; Ceramic electrolyte; Sintering.

## ANÁLISE DA SINTERIZAÇÃO DO ELETRÓLITO ZEI-8 CORRELACIONADA AO DESEMPENHO ELÉTRICO

### Resumo

O conhecimento dos mecanismos de densificação e sinterização de zircônia estabilizada com ítria (ZEI), o principal eletrólito de células a combustível de óxido sólido, é a base para o aperfeiçoamento de sua microestrutura. O presente trabalho tem por objetivo estudar os processos de sinterização e densificação, com base em análises dilatométricas, de ZEI dopada com 8% molar de ítria, produzida a partir de pós sintetizados por dois métodos (processo de combustão e método de Pechini), correlacionando o desenvolvimento microestrutural com o desempenho elétrico do material. Difração de raios-X e microscopia eletrônica de varredura foram usadas para caracterização microestrutural. Foram obtidas amostras com elevado grau de densificação e aquelas produzidas pelo método de Pechini apresentaram maior densificação no estágio final da sinterização e resultaram em cerâmicas mais densas e com melhor comportamento elétrico.

**Palavras-chave:** Zircônia estabilizada com ítria; Eletrólito cerâmico; Sinterização.

<sup>1</sup> Technical contribution to 65<sup>th</sup> ABM Annual Congress, July, 26<sup>th</sup> to 30<sup>th</sup>, 2010, Rio de Janeiro, RJ, Brazil.

<sup>2</sup> M.Sc., Doctoral student, Special Technologies Department (DTE), Electric Power Research Center, CEPTEL, P.O.Box 68007, 21940-970, Rio de Janeiro, Brazil. e-mail: csilva@cepel.br

<sup>3</sup> D.Sc., Professor, Department of Metallurgical and Materials Engineering, Federal University of Rio de Janeiro, P.O.Box 68505, 21945-970, Rio de Janeiro, Brazil. e-mail: pmiranda@labh2.coppe.ufrj.br

<sup>4</sup> D.Sc., Researcher, Special Technologies Department (DTE), Electric Power Research Center, CEPTEL, P.O.Box 68007, 21940-970, Rio de Janeiro, Brazil. e-mail: furtado@cepel.br

## 1 INTRODUCTION

Solid oxide fuel cell (SOFC), one of the types of fuel cells, is one of the most promising technologies for the production of energy, with potential to be a typical future distributed cogeneration system.<sup>(1-3)</sup> Typically, a SOFC system is constituted of at least seven distinct components: fuel feed, anode, electrolyte media (separating the two electrodes), cathode, oxidant agent feed (normally air), and electrical interconnectors (completing the electrical circuit) as schematically showed in the Figure 1.

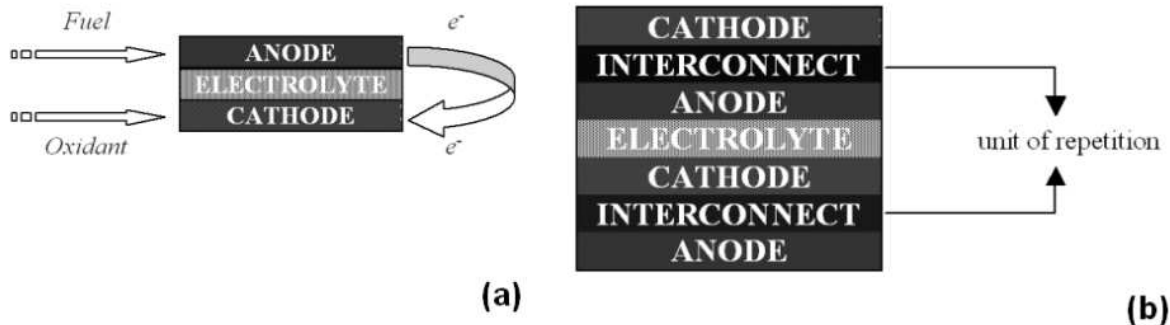


**Figure 1.** (a) Schematic diagram of a fuel cell; (b) scheme of the connection of the anode of a single fuel cell to the cathode of the subsequent single fuel cell, constituting a solid oxide fuel cell stack.

The efficiency of energy conversion of a SOFC and its performance durability mainly depend on the oxide ion conducting solid electrolyte activity.<sup>(4)</sup> In this context, the yttria-stabilized zirconia (YSZ) is one of the most popular materials employed as electrolyte in solid oxide fuel cell due to its pure oxygen-ion conductivity, good chemical compatibility, excellent mechanical properties, stability in dual environment (oxidizing and reducing) and thermal stability.<sup>(1,5)</sup>

YSZ is a versatile ceramic, which has found application in SOFC systems, oxygen gas and pH (hydrogen potential) sensors, oxygen pumps, thermal-barrier coatings, as a buffer layer of superconducting films, in components of electronic integrated circuits and in optical devices. In YSZ ceramics the oxygen vacancies are generated in the material to maintain electrical neutrality, since that the tetravalent zirconium ions are replaced by trivalent yttrium ions. Thus, two  $Y^{3+}$  ions correspond to an anionic oxygen vacancy, which it is responsible for the oxygen ion conductivity.<sup>(4)</sup>

An important requirement for a SOFC electrolyte material is its high density (low porosity). The sample's density influences its electrical and mechanical properties and, especially, increasing its ionic conductivity.<sup>(6)</sup> However, it is difficult to obtain a dense yttria stabilized zirconia ceramic.<sup>(5,7)</sup> Thus, the aim of this work is to characterize and evaluate the microstructural densification of bulk YSZ materials prepared from chemical synthesized powders, based on results from dilatometry experiments and contribute to the understanding of the processes of densification and sintering of this material.

## 2 EXPERIMENTAL

Figure 2 shows the preparation procedure of 8YSZ by both studied methods. For the combustion synthesis of 8mol% $Y_2O_3$ -stabilized zirconia (8YSZ) powder, by glycine-nitrate process (GNP), zirconyl nitrate hydrate ( $ZrO(NO_3)_2 \cdot 6H_2O$ , Acros

Organics, 99.5%), yttrium nitrate ( $Y(NO_3)_3 \cdot 6H_2O$ , Acros Organics, 99.9%) and glycine (Vetec) were dissolved in small amount of water. The homogeneous powder mixture, with glycine/metal oxides ratio equal to 2, was heated on a hot plate at 150°C and it was converted to a viscous gel due to evaporation of water. The mixture was then heated in a muffle furnace at 600°C until self-ignition. For the synthesis by Pechini's method, the zirconium oxychloride octahydrate ( $ZrOCl_2 \cdot 8H_2O$ ) and the yttrium nitrate pentahydrate ( $Y(NO_3)_3 \cdot 5H_2O$ ) were dissolved in ethylene glycol, anhydrous citric acid was added in a molar ratio of 1:5 between ethylene glycol and citric acid. The mixture was stirred for about 30 minutes under heating to 80°C, to promote polyesterification. The resulting gel was kept in oven at 180°C for 12 hours. The resulting fine powders were calcined at 900°C for 6h using heating rates of 10°C/min, with air flow rate of 60 mL/min. The powder was pressed into pellets of 12.4 mm in diameter and 2.1 mm in thickness at a pressure of 200 MPa.

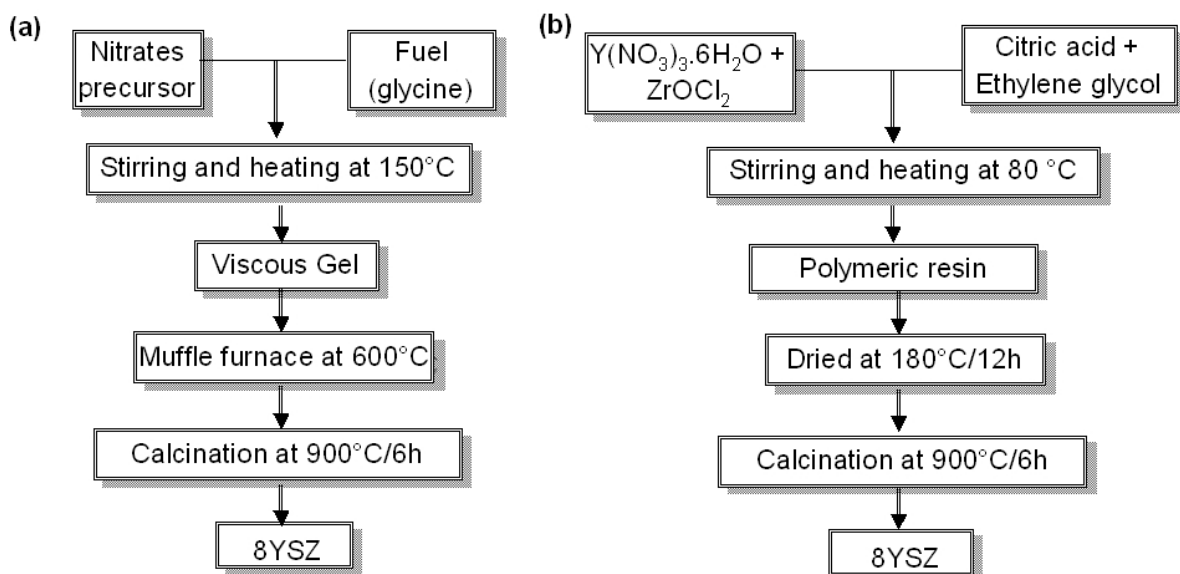


Figure 2. Preparation procedure of 8YSZ by (a) Combustion process and (b) Pechini method.

Sintering of the green compacts was performed in a thermo-dilatometer (Netzsch STA 402/409E) up to 1.550°C in air under non-isothermal conditions with 3°C/min heating rate, and cooled to room temperature. After measurement of the anisotropic coefficient (measurement of the shrinkage in 2 perpendicular directions) the linear shrinkage as a function of temperature, was used to trace the instantaneous densification normalized rate  $((1/\rho)dp/dt)$  – where  $\rho$  is the instantaneous density and  $t$  is the time – as a function of the degree of advancement of the densification (relative density) with respect to the theoretical density of the 8YSZ. The results of dilatometry tests presented below represent the average behavior of four samples.

Crystalline phase evolution of the resulted powder was detected by X-ray diffraction (XRD) analysis with a PANalytical X'Pert PRO diffractometer using Cu K $\alpha$  radiation ( $\lambda = 1.541806\text{\AA}$ ) with Ni filter and the data were collected from 20° to 100°. The microstructures of the densified samples were examined by scanning electron microscopy (SEM, Jeol JSM-64602 LV) equipped with X-ray dispersive energy spectroscopy (EDS, Link ISIS, Oxford Instruments) for compositional analysis. The final sintered discs were polished and thermal etched for 20 min at a temperature 50°C below the sintering temperature used. The density of the sintered sample was

measured by the Archimedes method (Mettler AE-200 analytical balance) using distilled water.

In the present work, investigations on the densification and sintering processes that occur in YSZ were made based on the phenomenological approach developed by Su and Johnson<sup>(8, 9)</sup> and Hansen,<sup>(10)</sup> which presents a great advantage over the models that preceded it, because it enables the determination of apparent activation energy of sintering regardless of the mechanisms involved in the process and during the whole process of sintering. The relation between the geometric factors and relative density (or densification degree,  $\rho(t)$ ), at time  $t$ , is obtained through the expression:

$$\rho(t) = \frac{\left(1 + \frac{(L_f - L_i)}{L_i}\right) \left(1 + \frac{(d_f - d_i)}{d_i}\right)^2}{\left(1 + \frac{\Delta L(t)}{L_i}\right) \left(1 + \left[\frac{(d_f - d_i)L_i}{(L_f - L_i)d_i}\right] \frac{\Delta L(t)}{L_i}\right)^2} \rho_f \quad (\text{Eq.1}),$$

where  $L_i$  and  $L_f$  are, respectively, the initial and final lengths of the samples,  $d_i$  and  $d_f$  are, respectively, the initial and final diameter of the samples,  $\Delta L = L_f - L_i$  and  $\rho_f$  is the final relative density of the sample considered.

Based on this approach we can then consider the problem of densification of ceramic materials, to obtain the densification rate as a function of the densification degree (relative density). Furthermore, the time-normalized gradient of the linear shrinkage, obtained under isotherm conditions, is the same as that found under non-isothermal conditions<sup>(8-10)</sup>. This makes it possible to group the set of kinetic (time) and thermal (energy) parameters in the global function  $\Theta(t, T)$ , defined as:

$$\Theta(t, T) = \int_{t=0}^t \frac{1}{T} \exp\left(-\frac{Q_s}{RT}\right) dt \quad (\text{Eq.2}),$$

where  $Q_s$  is the apparent activation energy of the sintering process,  $T$  is the absolute temperature and  $R$  is the ideal universal gas constant.

Electrical conductivity measurements were carried out by Keithley 614 electrometer and silver paint was used as electrode material for electrical measurements. The presented results of electrical measurements are the average value of four samples.

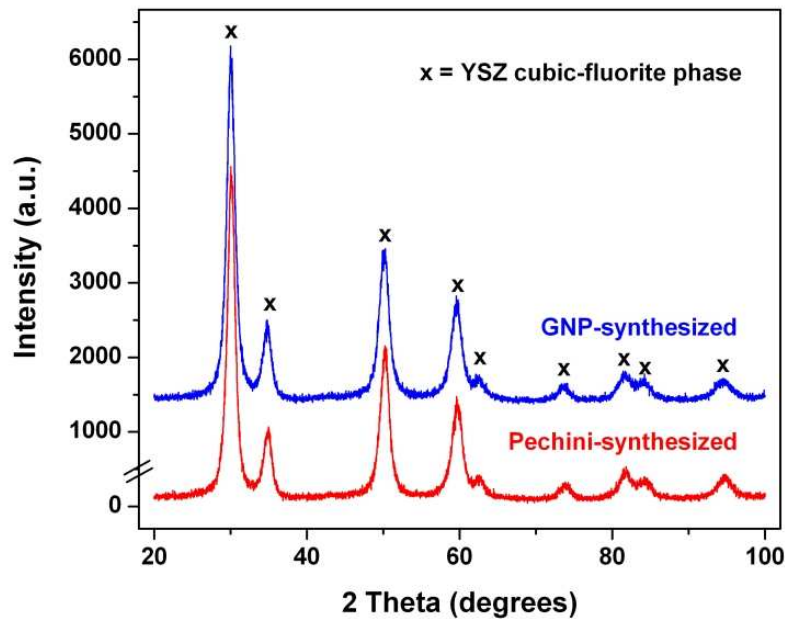
### 3 RESULTS AND DISCUSSION

Figure 3 shows the X-ray diffraction patterns of 8 mol% yttria-stabilized zirconia (8YSZ) powders synthesized by the glycine-nitrate process (GNP), a combustion synthesis method, with oxide and glycine ratio equal to 2, and by the Pechini synthesis method. As shown in Figure 2, a good crystallite state was observed for both samples after calcination, indicating the formation of a single-crystalline cubic phase, according to 030-1468 JCPDS card. The calculated 'd' values match with the reported yttria stabilized cubic zirconia having a composition  $Y_{0.15}Zr_{0.85}O_{1.93}$  and the lattice parameter 'a' was estimated to be 5.139 Å. Approximate crystallite sizes were calculated using data from the X-ray diffraction

patterns and the Scherrer's equation (Eq. 3) based on full width at half maximum (FWHM) of c-YSZ (111) peaks.

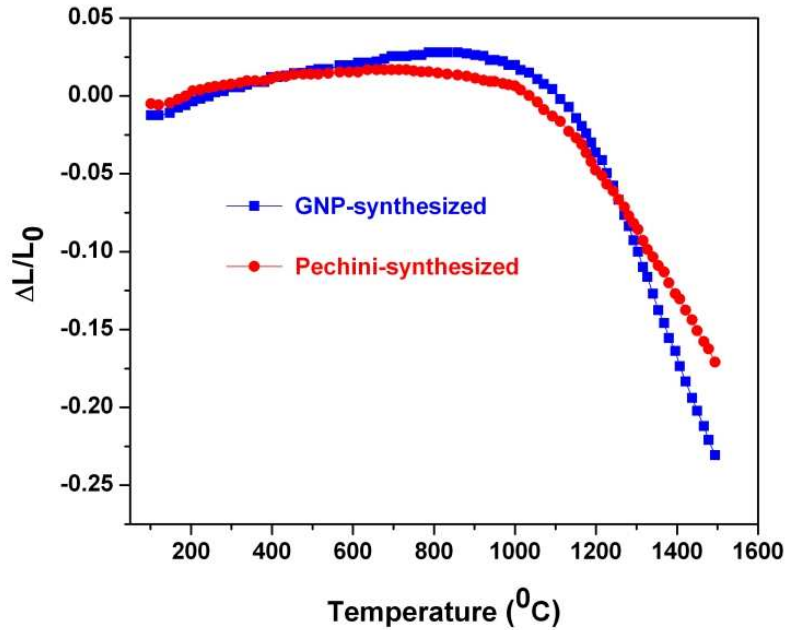
$$L = 0.9 \lambda / (\beta \cdot \cos\theta) \quad (\text{Eq.3})$$

Where L is the crystallite size,  $\lambda$  is the wavelength of the filament used in the XRD machine,  $\beta$  is the width of a peak at half of its intensity and  $\theta$  is the diffraction angle of the same peak. The average crystallite sizes calculated for each sample were  $(6.1 \pm 1.5)\text{nm}$  for the GNP-synthesized powder and  $(13.2 \pm 3.2)\text{nm}$  for the Pechini-synthesized powder.



**Figure 3.** Powder X-ray diffraction patterns of 8YSZ calcined samples.

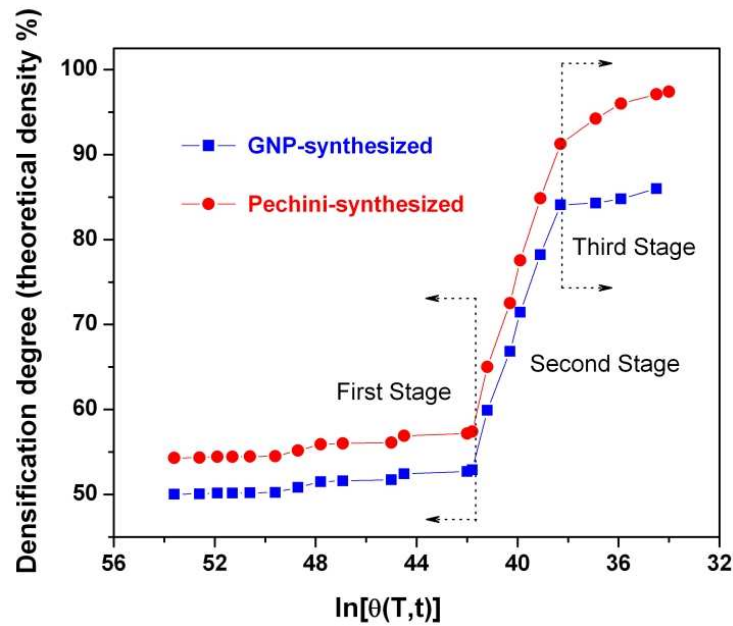
Figure 4 shows the average shrinkage data with respect to the change in temperature. These shrinkage results do not show any discrepancy from what is generally expected for such material types of testing and is therefore accepted as reliable for further densification profiles analysis.<sup>(11)</sup> The GNP-synthesized 8YSZ presented a total shrinkage of about 24%, while the 8YSZ samples synthesized by the Pechini's method exhibited a total shrinkage of about 18%. Additionally, it is noted that in both cases the 8YSZ green compacts start to shrink at approximately 1.000°C and they do not finish up to 1.500°C.



**Figure 4.** Linear shrinkage curves for the 8YSZ pellets.

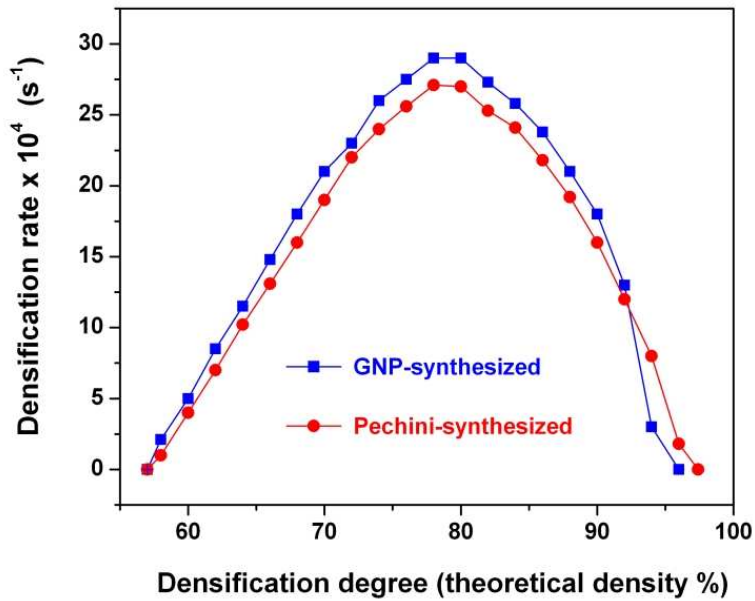
Based on these dilatometric test results it has been possible to study the thermo-temporal behavior of 8YSZ samples during sintering. Figures 5 and 6 present respectively the results on the master sintering curves and of the densification rate as a function of the densification degree of the 8YSZ samples studied.

According to the curves shown in Figure 5, the average behavior of the densification evolution during the first stage of sintering (which presents no significant increase in relative density) is very similar either for the 8YSZ that was synthesized by the GNP or for that obtained by the Pechini method. However, throughout this stage, the relative density profile is about 10% higher for the system synthesized by the Pechini method. In the second stage the angular coefficients of the straight lines that describe the increasing of the densification degree are essentially equal for both curves, indicating the occurrence of the same sintering mechanism.<sup>(11)</sup> Moreover, in the third stage of sintering, there is a significant difference in behavior, showing that the system synthesized by the Pechini method still presents a considerable gain in its relative density, unlike what happens with the system synthesized by the GNP, which certainly can be attributed to the different intrinsic characteristics of the ceramic powders.<sup>(12)</sup>



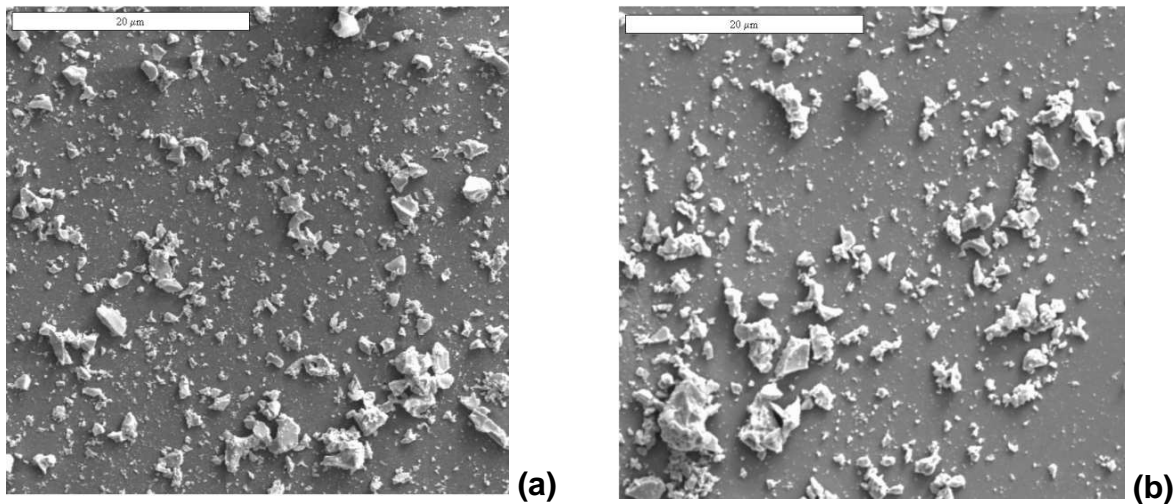
**Figure 5.** Microstructure evolution (master sintering curves) for the 8YSZ samples studied.

Additionally, Figure 6 shows the curves of densification rate as a function of the densification degree (relative density) for the 8YSZ systems studied. It is clear that in the beginning (green body density) up to about 90% of the theoretical density, the evolved mechanisms are essentially the same, although the densification kinetics of the GNP-synthesized powders has been slightly faster than the powder synthesized by the Pechini method. In fact, the initial slopes are almost identical for the two powder systems studied. This situation reverses after about 93% of densification degree is attained, already in the decreasing part of the curves, then when it seems that the densification rate of the GNP-synthesized system becomes slow. This observation corroborates the results presented in the graphs of Figure 5, especially for the third stage of sintering, when the Pechini-synthesized system still keeps significant densification increment. However, in the final stage, the behaviours were similar. The final relative densities achieved ( $98.4 \pm 0.4\%$ ) and ( $96.9 \pm 0.8\%$ ), percentages of the theoretical density, respectively for the Pechini-synthesized and GNP-synthesized samples, are also consistent with those determined by the Archimedes method.



**Figure 6.** Densification rate as a function of the densification degree (relative density) for the 8YSZ samples studied.

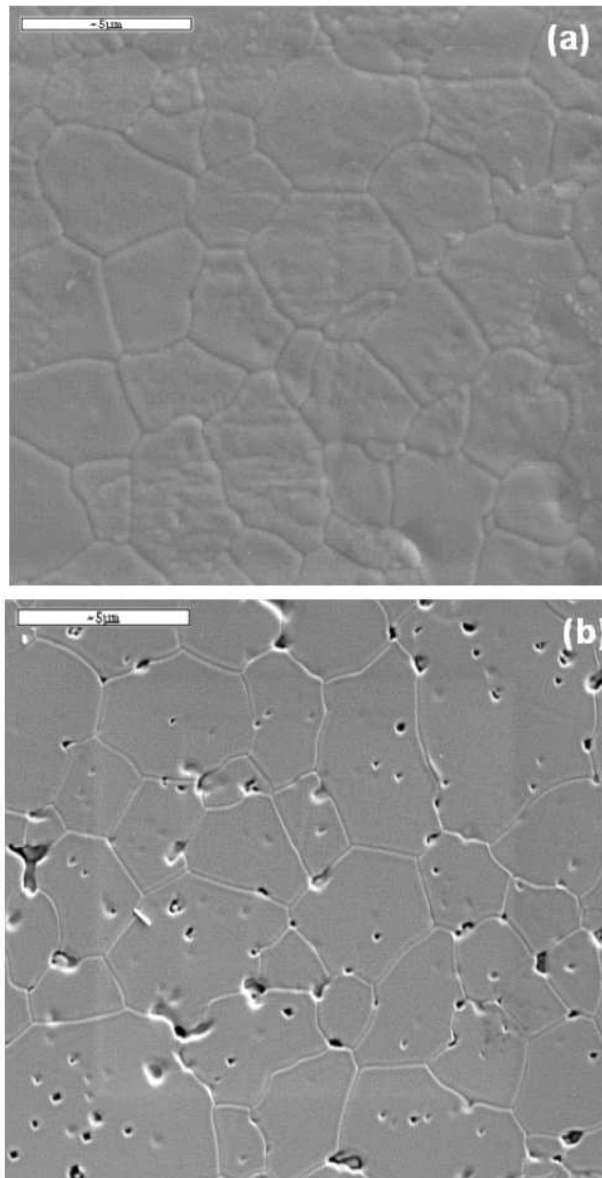
Figure 7 shows examples of morphological characteristics of the powder mixtures examined by a scanning electron microscope which reveals that, for the both synthesis methods investigated, there are fine particles with non-ideal spherical shape, despite the results of densification have been good, suggesting the formation of weak aggregates.



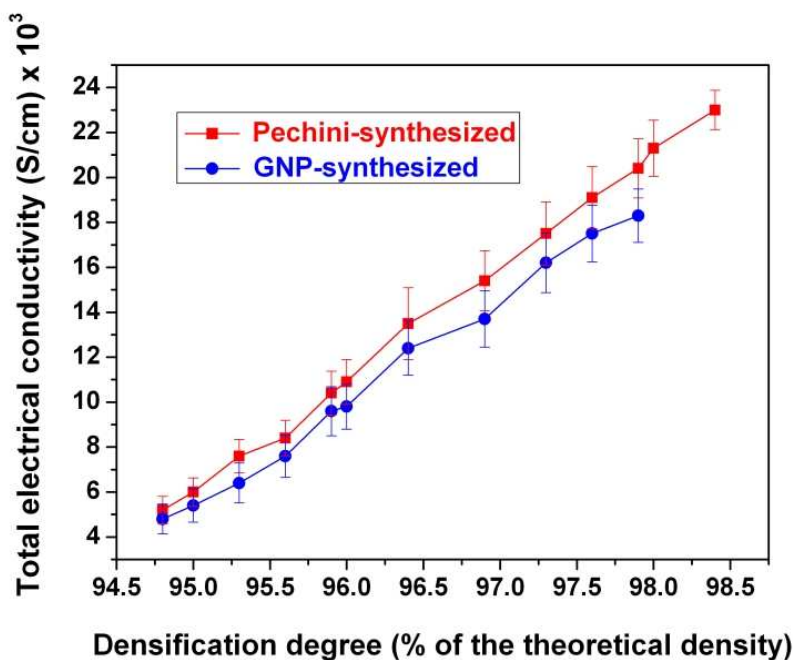
**Figure 7.** SEM micrographs of 8YSZ powders produced by: (a) Pechini method; (b) GNP.

Figure 8 shows the thermal etched surface images of the sintered pellets studied. As shown in Figure 8, in both cases, the grain boundaries were clearly identified, and grain size distributions are similar, with average grain size about 3  $\mu\text{m}$ . In addition, it was found that the 8YSZ Pechini-synthesized sample pellet presented a fully densified microstructure, with absence of porosities. Already the microstructure of the GNP-synthesized pellet shows intra and intergranular porosity, which is more consistent with its most densification speed, since that possibly this condition did not provide the time needed for complete elimination of pores, as also observed by Wang *et al.*<sup>(12)</sup> However, this sample also shows clear grain boundaries.

Figure 9 shows the curves that expressing the relationship between the total electrical conductivity as function of the densification degree (relative density) for the 8YSZ samples studied. It was noted that in general, along of all the range of densification degree the average total electrical conductivity of the samples synthesized by the Pechini method is higher than that of samples obtained by GNP (on average, about 10%). Additionally, note that the behavior of electrical conductivity in relation to degree of densification is very similar for both systems studied. Indeed, as shown in Figure 8, the highest level of porosity of the samples obtained by GNP makes harder the electric transport (ionic) in the sintered material.<sup>(13,14)</sup> The best results are of the order of 0.02 S/cm.



**Figure 8.** SEM micrographs of sintered 8YSZ specimens, after thermal etching, which powders were produced by: (a) Pechini method; (b) GNP.



**Figure 9.** Total electrical conductivity as function of the densification degree (relative density) for the 8YSZ samples studied.

#### 4 CONCLUSIONS

This study examined dilatometric sintering experiments performed with nanostructured 8 mol% yttria stabilized zirconia ceramic powders and identified the sintering density evolution profiles of samples whose precursor powders were synthesized by two different methods (glycine-nitrate process and Pechini's method). It concluded that the same mechanisms of sintering are present in the sintering behaviour of both systems studied. Three stages of sintering were identified and it was found that the samples obtained by the Pechini's method showed a higher densification degree in the final stage of sintering, slower densification kinetics and resulted in ceramics with higher final relative density. Additionally, it was found that the dependence of total electrical conductivity in relation to the densification degree is very similar for the samples synthesized by the two processes studied and the best results of electrical conductivity are of the order of 0.02 S/cm.

#### REFERENCES

- 1 O'HAYRE, R.; CHA, S-W.; COLELLA, W. Fuel Cell Fundamentals. John Wiley & Sons, 2009.
- 2 NEEF, H.-J. International overview of hydrogen and fuel cell research. Energy, V. 34, p. 327-333, March 2009.
- 3 ZINK, F; LU, Y.; SCHAEFER, L. A solid oxide fuel cell system for buildings. Energy Conversion and Management, V. 48, p. 809-818, March 2007.
- 4 YOKOKAWA, H.; TU, H.; IWANSCHITZ, B.; MAI, A. Fundamental mechanisms limiting solid oxide fuel cell durability. Journal of Power Sources, V. 182, p. 400-412, 1 August 2008.
- 5 STEELE, B. C. H.; HEINZEL, A. Materials for fuel-cell technologies. Nature, V. 414, p. 345-352, 2001.
- 6 GHATEE, M.; SHARIAT, M. H.; IRVINE, J.T.S. Investigation of electrical and mechanical properties of 3YSZ/8YSZ composite electrolytes. Solid State Ionics, V. 180, p. 57-62, February 2009.

- 7 SILVA, C. A.; RIBEIRO, N. F. P.; FURTADO, J. G. M.; SOUZA, M. M. V. M. A study on densification of yttria-stabilized zirconia synthesized from glycine-nitrate process and sintered under different conditions. Proceedings of the Annual Meeting of the Brazilian Metallurgical and Materials Association, Santos, Brazil, July 2008.
- 8 SU, H.; JOHNSON, D. L. Master Sintering Curve: a practical approach to sintering. Journal of the American Ceramic Society, V. 79, p. 3211-3217, 1996.
- 9 SU, H.; JOHNSON, D. L. Master Sintering Curve. Rational Design and Processing of Advanced Ceramics Workshop, NIST, 1995.
- 10 HANSEN, J. D.; RUSIN, R. P.; TENG, M-H.; JOHNSON, D. L. Combined-stage sintering model. Journal of the American Ceramic Society, V. 75, p. 1129-1135, 1992.
- 11 MAZAHERI, M. M.; VALEFI, M.; HESABI, Z. R.; SADRNEZHAAD, S.K. Two-step sintering of nanocrystalline  $8Y_2O_3$  stabilized  $ZrO_2$  synthesized by glycine nitrate process. Ceramics International, V. 35, p. 13-20, January 2009.
- 12 WANG, Q.; PENG, R.; XIA, C.; ZHU, W.; WANG, H. Characteristics of YSZ synthesized with a glycine-nitrate process. Ceramics International, V. 34, p. 1773-1778, September 2008.
- 13 ZHANG, T.S.; CHAN, S.H.; WANG, W.; HBAIEB, K.; KONG, L.B.; MA, J. Effect of Mn addition on the densification, grain growth and ionic conductivity of pure and  $SiO_2$ -containing 8YSZ electrolytes. Solid State Ionics, V. 180, p. 82-89, February 2009.
- 14 LI, Q.; XIA, T.; LIU, X.D.; MA, X.F.; MENG, J.; CAO, X.Q. Fast densification and electrical conductivity of yttria-stabilized zirconia nanoceramics. Materials Science and Engineering B, V. 138, p. 78-83, March 2007.